Imperial College London

"A real-time intraoperative data mapping device for probe-based measurement using computer vision"

Hyunggi Chang

"A thesis submitted in partial fulfilment of the requirements for the degree of MRes in Medical Robotics and Image Guided Intervention and for the Diploma of Imperial College"

Imperial College London

September, 2018

Supervised by Fernando Avila-Rencoret and Professor Daniel Elson

Acknowledgements

I would like to acknowledge everyone who has supported me throughout this MRes project.

First, I would like to express my special gratitude to my supervisors: **Professor Daniel Elson** and **Fernando Avila-Rencoret**. Professor Daniel Elson has made sure the direction of my research goes the most efficient and the productive method throughout the project. He also shared his wide insight towards biomedical optics, which greatly inspired me in and out of the project. Fernando Avila-Rencoret has helped me in understanding research methodology and making effective communication of data with other researchers. With the support from the two supervisors, I had an amazing experience to delve into the field of biophotonics and computer vision.

I also would like to acknowledge the **members of Project OpenPath**. This project allowed me to have a wide insight over the field before I started the project.

Also, I would like to express my thanks to **Alexandros Kogkas**, who helped me with understanding of computer vision and multiview geometry, **Ya-Yen Tsai**, who introduced me to OpenCV, **Maria Leiloglou**, who shared her knowledge about optics and hyperspectral methods, and **Qing-biao Li**, who helped me in MATLAB programming problems.

Most of all, I would like to express my best thanks to **my family** for supporting me always.

Table of Contents

Abbreviations

AFI – Autofluorescence Imaging

CLM – Confocal Laser Microscopy

DRS – Diffuse Reflectance Spectroscopy

FI – Fluorescence Imaging

FLIM – Fluorescence Lifetime Imaging Microscopy

FOV – Field of View

IMA – Intraoperative Margin Assessment

MSOT – Multispectral Optoacoustic Tomography

NBI – Narrow Band Imaging

OCT – Optical Coherence Tomography

PET – Positron Emission Tomography

QFD – Quality Function Deployment

RS – Raman Spectroscopy

VOC – Voice of Customer

1 Introduction and Literature Review

1.1 Curative Cancer Surgery

Curative cancer surgery is one of the main cancer treatment procedures, which can be performed alone or in combination with perioperative radiotherapy or chemotherapy. Surgery is effective in curing different types of non-haematological cancers by removing the entire localised tumours, before set up of no new malignant tumour colonies at distant tissues prior to the surgery (cancer metastasis) [1].

There are two main goals for the curative cancer surgery: first goal is to **remove all malignant tumour tissues from the body**, and second is to **conserve as much healthy tissue as possible to keep healthy tissue physiology and function** [2].

Removal of entire malignant tumour tissue in the body prevents serious biological malfunctions by stopping the local invasion of the cancerous tumour or growth into the nearby healthy tissues [3]. During the surgery, surgeons may require to perform elimination of adjacent lymph node to prevent the chance of metastasis in case of presence of cancer cells at the lymph node [4]. It is important to execute a complete removal of all malignant cancerous tissue during the surgery, because due to limitless growth of malignant cancer. Small cancer residue from incomplete tumour removal can lead to local recurrence of cancer even at microscopic level [5]. This leads to concern on distinguishing margins for cancerous cells from normal healthy tissues.

Surgeons must excise the tumour with a sufficient range of margin for the surrounding healthy tissues. The margin status is generally categorised into 3 classes: **Positive margin**, **Negative margin** and **Close margin**.

Positive margin: There is presence of invasive or premalignant cancer cells at the surgical resection line. A positive margin represents presence of invasive cancer residue at the excision point, therefore more tissue needs to be removed.

Negative margin: There is no presence of cancer cells at the surgical resection line. A negative margin may represent a complete removal of invasive or pre-malignant cancer at the excision point.

Close margin: There is presence of cancer cells very close to the surgical resection line, which makes difficult to determine if cancerous tissue is completely removed from the local site.

Negative margins are desired in cancer surgeries for patients' benefits and economic use of resources and time. Previous studies have shown that failed in margin control (i.e. positive margins and close margins with incomplete cancer removals) is a risk factor for local recurrence of cancer on soft-tissue sarcoma, renal cancers, and prostate cancers [6]–[8]. Local recurrence has a strong correlation to mortality rates and prognosis on survival to a certain extent. This was evident from research data with pointed out local recurrences on soft-tissue sarcoma, colorectal cancer and hepatic cancer have significantly decreased overall survival [9]–[12], and in the case of oesophageal cancer, the mortality rate was double in positive compared to negative resection margins [2]. Local recurrences can cause extra economical cost, for a requirement of further require re-excision and / or adjuvant therapy. Abe *et al* suggests that re-excision due to local recurrence has predicted cost of $18.8 million per year, excluding hospital costs, the cost of surgical complications after re-excision [13].

However, many researchers agree that late staged cancer or large sized tumours are stronger reasons for mortality than local recurrences [6], [9], [10], [14]. In the case for breast cancer surgeries, local recurrence showed no effects in disease-specific survival [14]. This shows that the effects of local recurrences may vary depending on the impacts of tumour resection and levels of surgical complications for post-recurrence therapies for different types of cancer.

To maximise postoperative physical function in patient, preservation of healthy tissue from surgical location must be achieved during curative cancer surgery. A large resection margin ensures increased chance of attainment of a negative margin. This may successfully prevent local

recurrence hence it may lead to further unnecessary clinical issues in patients – functional disorders of sphincter function disorder was found in resecting low rectal tumours [15], and delayed gastric emptying and dumping syndrome were found in esophagectomy [16].

In order to balance the two competing goals, numerous intraoperative margin assessment (IMA) method has been established to determine the margin status accurately. However, despite the technological advance, margin positivity still remained as a same significant obstacle in curative cancer surgery over the past few decades, causing recurrences [17] – the margin positivity have remained consistently above 15%, up to 60% [18]–[23].

1.2 Intraoperative Margin Assessment (IMA)

Prior to the surgery, preoperative imaging modalities like CT, MRI, PET/CT are used to confirm the tumour locations and plan the surgery. Although there have been successful attempts in developing systems for registering preoperative data on intraoperative settings in real-time [24]–[26], the robustness and the cost-effectiveness has not been shown to be commercially available.

During the surgery, surgeon's vision is not accurate enough to determine if all invasive cancer cells have been removed. Certain types of cancerous tumours are visually indistinguishable from the surrounding healthy tissues, which calls a need for a tissue diagnosing modality. Also, for the types of cancerous tumours that visually stands out from the surrounding tissue, it is difficult to determine if all cancer cells at microscopic level have been removed – this calls a need for a microscopic cell analysis. Therefore, an accurate intraoperative margin assessment (IMA) method still is a requirement for modern cancer surgeries.

The current standard of care dictates that any lesions that are discovered during preoperative scans and that are visually inspected during the surgery, are to be removed for biopsy [27]. This is because the tissue type can only be identified through histopathological analysis. The biopsy site is chosen by a subjective decision unless a skilled pathologist is accompanied to assist, hence there is a **risk of sampling error** when the surgeon alone takes the biopsies. In the case of

diagnosis of Barrett's oesophagus, there have been cases resulting false negatives due to incorrect sampling [28].

The biopsy is then analysed by a pathologist at the hospital lab, using Frozen Section or Imprint Cytology methods [29]. If the pathology lab is equipped with Faxitron histoscanner, it may use Faxitron analysis, which combines conventional radiography feature for detecting micro-calcification to histopathological analysis [30]. However, this method is not widely adopted.

Both frozen section and imprint cytology have certain **inherent errors within the analysis phase**. Frozen section method involves analysing a cryo-section of the tissue, which allows for a rapid microscopic examination. This method suffers from false identification of signet ring pathology, and also it is reported that ductal carcinoma *in situ* and benign lesions like intraductal papilloma change its morphological structure upon freezing [31]. Imprint Cytology involves touch-imprinting or scraping the specimen surface to be examined under the microscope. This method suffers from false identification of dense fibrous stroma as tumour, which accounts for 6% of false positives [32]. Suen *et al* recommends using a combination of frozen section and imprint cytology method to avoid inherent interpretation errors, but this suggestion is impractical due to the cost and time required for dual-modality analysis [32].

Risks of human errors may also appear in the results, since the analysis and interpretation of microscopic data relies on visual inspection. Figure 1 shows an example of carcinoid for a renal cancer surgery, and the only way to determine presence of cancer is the pathologist's knowledge and visual inspection skills. Due to this, the outcome may suffer from **intra-pathologist and inter-pathologist variability**, which may differ by individual's skills and experience, as well as working condition of the pathologist [33]. Google Brain has attempted to reduce this variability, by adopting artificial intelligence to automatically analyse pathology images using convolutional neural network and provide visual guide using augmented reality [34]. However this system has not been publicly nor commercially released.

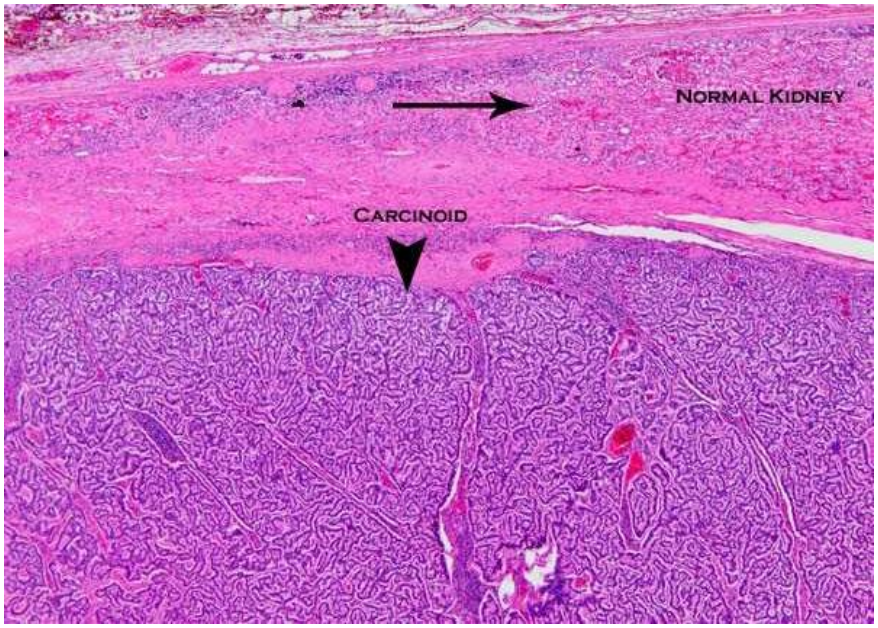

Figure 1 histopathology image of renal carcinoid [35]

Additionally**, the absence of spatial information of histopathology analysis may lead to unnecessary removal of healthy tissues**. The report back to the theatre usually only reveals whether there is invasive or premalignant cancer cells present at the resection plane. In the case of a confirmed presence of cancer cells at the resection plane, the healthy tissue at the excision point needs to be further excised in all directions, since the analysis result does not instruct in which orientation the cancer cell lies. If spatial information was provided to instruct the exact location of the cancer cells on the biopsy, less healthy tissue may be removed to achieve negative margin.

Also, there is a **risk of human error in matching the result from the histopathology analysis to the correct excision location**. False matching of biopsy result to the biopsy location may lead to leaving pre/malignant cancer cells in the body, which may lead to local recurrence and re-excision consequentially, while removing unnecessary healthy tissues at a wrong biopsy location.

MODALITY	FROZEN SECTION	IMPRINT CYTOLOGY
SENSITIVITY	86%	91%
SPECIFICITY	96%	95%

Table 1 sensitivity and specificity of frozen section and imprint cytology [29]

Table 1 shows that frozen section and imprint cytology methods show a good accuracy in general despite some misinterpretation errors, however, **the entire process of analysis is time-consuming**. As shown from Figure 2, the process of taking the biopsy, transporting it to the lab, preparing for analysis, performing histopathological analysis, and bringing the report back to the surgical theatre, takes up to 29 minutes average per biopsy. This causes a cancer surgery consisting of removing multiple localised tumours take up to 8~9 hours on average [36].

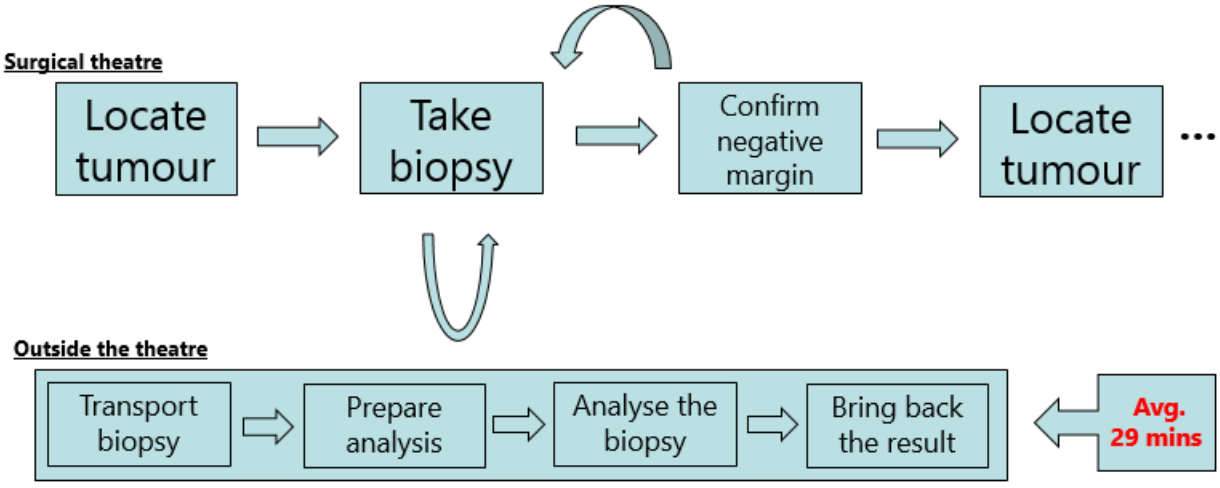

Figure 2 Process flowchart of biopsy analysis

Also, a large proportion of biopsies sent to the pathology lab have been confirmed as benign, especially in the case of polypectomy, 40% of colonic polyps have been identified as benign [37], which means the tissue could have been left *in situ*, and **resources and time have been wasted in identifying harmless tissues**.

Additionally, while waiting for the analysis result to come back to the surgical theatre, the patient must serve idle time, which leads to **patient discomfort**, **occupancy of operating theatre**, and

increased operation cost. Also, the associated cost in **analysis equipment**, **time**, and **personnel** are very expensive, which could have been allocated for other tasks that the pathology lab assists on. Studies show that the use of frozen section and imprint cytology for margin assessment provide cost savings only when the re-excision rates are greater than 36% [38]. For these reasons, it is reported that none of the 18 breast screening centres in London routinely use frozen section or imprint cytology for margin assessment in 2017 [29].

Despite the method being a clinical gold standard, the inefficiency of the process does not allow it to be used routinely. Clearly, there is a need for modification to reduce the inefficiency within the IMA process using frozen section and imprint cytology methods. Process improvement method, Design for Six Sigma (DFSS) states that there are seven types of wastes within an inefficient process: transport, inventory, waiting, over-processing, over-production and defect [39].

The following wastes are found in this process:

- **Transport –** Transporting the biopsy to the pathology lab does not create any values for the goal of surgery. The resources, time and personnel spent for the transport are wasted, and could have been allocated elsewhere.
- **Motion** – Freezing / touch-imprinting / inking the biopsy does not create any value for the goal of surgery. The resources, time and personnel spent for the preparation are wasted, and could have been allocated elsewhere.
- **Waiting** – While waiting for the results to come back, idle time is being served at the theatre. Waiting creates no values for the goal of surgery.
- **Over-processing** – Spending time and effort in producing reports for effective communication between the pathology lab to the surgeon does not create any values for the goal of surgery.

- **Defects** – Sampling errors, inherent errors, intra/inter-pathologist variabilities, biopsy mismatch error reduces the performance of the surgery.

For the IMA process to be improved, the origin of these wastes needs to be identified, and then get eliminated or replaced by a better feature.

1.3 Problem Statement

Surgeons require an accurate assessment of tumour border for a complete cancer removal during curative cancer surgery. However, surgeons alone are not able to confirm the presence/absence of cancerous cells without assistance from the pathology lab [40].

The current methods to solve this problem, which the histopathological analysis via frozen section and imprint cytology methods at pathology labs, comprise of very inefficient processes, despite being considered as the gold standard procedure for IMA. The identified wastes from the previous section and its consequences could be clustered into four different origins, by using Ishikawa (Cause & Effect) analysis [41].

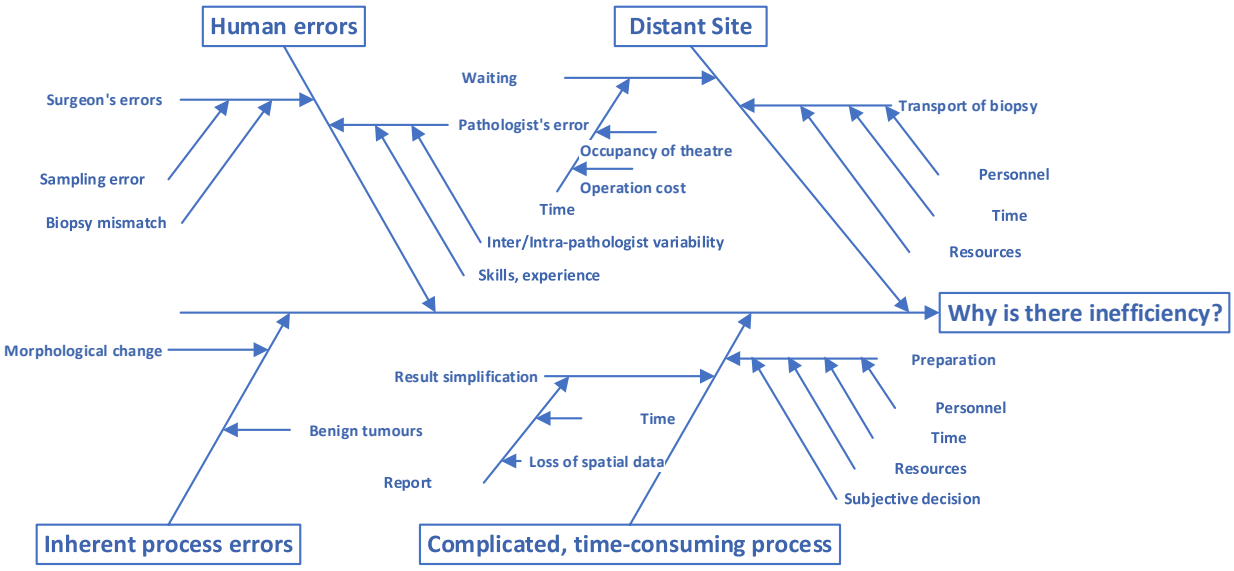

Figure 3 Ishikawa (Cause & Effect) diagram of inefficiency in current IMA methods

As shown on Figure 3, the inefficiency within the process mostly comes from the distant site of analysis, complicated and time-consuming processes of analysis, process inclusive of human errors, and inherent process errors.

1.3.1 Proposed Clinical Solution

To eliminates the wastes that were analysed in the previous section, a new process should be adapted to be better in achieving the ultimate goal of the process to improve patient benefits. To eliminate the wastes, the factors that generates wastes should be replaced with other features that solve the previous issues:

- 'Distant site of analysis' can be replaced with **'in-house / intraoperative system**'.
- 'Complicated and time-consuming process of analysis' can be replaced with **'real-time tissue analysis that the surgeon can use'.**
- 'Process inclusive of human errors' can be replaced with **'process comprising of quantitative analysis with spatial information'**.

The last type of waste, 'inherent process errors', cannot be replaced with a new feature, since the new system may also have its own inherent process errors. Therefore, the development is focused on minimising inherent process errors.

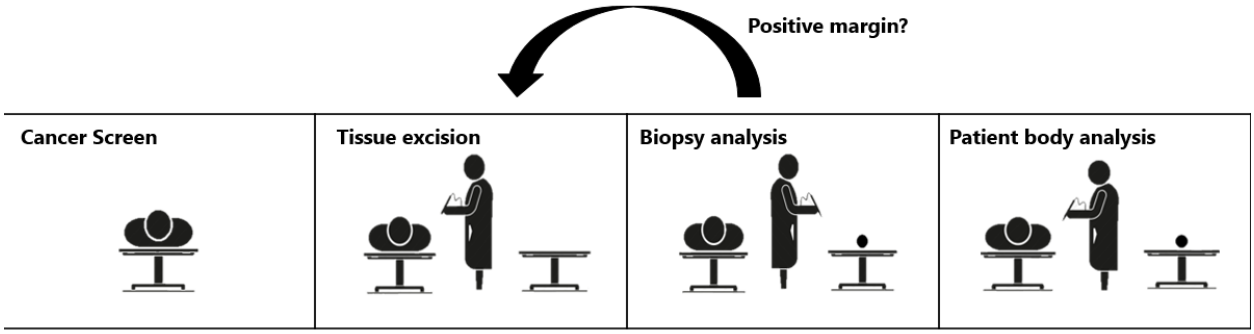

Figure 4 Proposed clinical solution

In whole, there is a need for an **in-house intraoperative real-time quantitative tissue diagnosis system with spatial information that surgeons can use alone**. With this system, a clinical

workflow can be assumed, as shown in Figure 4. The workflow starts with a preoperative imaging or red-flagging technologies like NBI [42], to briefly locate the tumour position in the body. Once the localised tumour is found, the surgeon uses the system to find the border between the cancerous tumour and the healthy tissue and excises the tumour with a small margin. The excised tissue is then transported to a tray, and then the surgeon looks for presence of any cancer cells at the resection plane of the excised tissue. If there is a sign of cancerous cells, then more tissue needs to be excised from the local excision point. Once absence of cancerous cells is confirmed at the resection plane, the surgeon searches for cancer residue on the patient body to confirm that all cancerous tissues are removed from the body.

1.3.2 Existing Solutions for Tissue Diagnosis

Although frozen section and imprint cytology methods are considered as the gold standard procedure for tissue diagnosis, there are other methods available both at commercial grade and at research level. Technological advances have allowed numerous imaging modalities to be used in tissue diagnosis, certain limitations such as associated cost or problematic integration with the clinical workflow have hindered the translation to the operational theatres. More details on each method can be found in Appendix I.

In-house histology scanner is a portable version of the histology scanner at the pathology lab. Commercial products by Leica [43] and SamanTree Medical [44] have been widely used in histopathology analysis outside the hospital. These devices have a potential to be used during curative cancer surgery, and therefore to eliminate the process of transporting the biopsy to the pathology lab. Also, there is no learning curve in using the equipment protocol-wise, since already known methods of frozen section and imprint cytology methods are repeated to be used. However, in-house histology scanner still requires the presence of a skilled pathologist during the entire surgery, and the inherent errors of frozen section and imprint cytology still affects the accuracy of outcome. This goes against our aim of performing real-time tissue diagnosis,

quantitative analysis with spatial information, and tissue diagnosis by the surgeon alone. Therefore, in-house histology scanners cannot be selected because they fail to meet our criteria.

Fluorescence Imaging (FI) [45]–[48], Fluorescence Lifetime Imaging Microscopy (FLIM) [49], Narrow Band Imaging (NBI) [50], [51], Autofluorescence Imaging (AFI) [52], Optical Coherence Tomography (OCT) [53]–[55] are non-contact based optical biopsy methods. FI and FLIM (in the case of using exogenous fluorophores) uses fluorescence emission from exogenous fluorophores that accumulate at cancer tissues. NBI and AFI captures specific wavelength of light at the scene that highlights the features of cancerous cells. OCT uses coherent light to achieve a micrometre-resolution, which then acts as a microscope. FI, FLIM, NBI, and AFI are able to use light intensity values at specific wavelength to quantitatively analyse the optical tissue characteristics, while still obtaining spatial information. The drawbacks of FI and FLIM (in the case of using exogenous fluorophores) are requiring injection of exogenous fluorophores, such as indocyanine-green (ICG), prior to surgery [56]. FI, FLIM, NBI, and AFI may be used for tissue diagnosis for our criteria, as they are able to highlight cancer tissues on 2D images, though NBI and AFI may need extra visualisation for surgeons to use alone. Surgeons then may use the highlighted 2D images as a visual guide for tumour excision. On the other hand, OCT does not fit in our criteria, as interpretation of microscopic images requires a skilled pathologist.

Contact-based non-optical approaches include analysing bioimpedance of tissues [57]–[59], detecting abnormally high metabolic activities by handheld Positron Emission Tomography (PET) [60], analysing molecular constituents of tissue by mass spectrometry [61]–[63], and analyse the tissue morphology using ultrasound. Contact-based approaches to deduct the tissue properties are comprised of interactions that may be destructive or harmful to the patient, to achieve the tissue properties. For example, PET exerts radiation exposure onto the tissue, and mass spectrometry disintegrates the tissue into molecular levels. PET and ultrasound method do not fit in our criteria, as interpretation of PET and ultrasound image requires an expert in field.

Bioimpedance method may suffer from a poor resolution compared to other methods, as the process of measuring the bioimpedance requires two electrodes that are separated by a certain extent, and this separation defines the resolution of the system [59]. Mass spectrometry method may suffer from its large equipment size and its expensive cost around $380,000 [64], and the absence of spatial information in the outcome. However, despite the drawbacks, bioimpedance and mass spectrometry still may fit in our criteria, since they can perform real-time quantitative analysis of tissue characteristics.

Contact-based optical biopsy method are *In situ* microscopy / confocal laser microscopy (CLM) [65], Raman spectroscopy (RS) [66]–[68], Multispectral Optoacoustic Tomography (MSOT) [69], and Diffuse Reflectance Spectroscopy (DRS) [70], [71]. Optical biopsy methods use only light (except MSOT, which combines ultrasound measurement with optical analysis) to interact with the tissue, so there is no tissue destruction. CLM may not fit into our criteria, since interpretation of high-resolution optical imaging requires the presence of a pathologist in site unless fluorescence guidance is provided. MSOT, for similarly, needs to be accompanied with the expertise of interpreting ultrasound images, therefore it may not fit into our criteria. RS and DRS provides spectroscopic data, which can be used for real-time analysis. However, due to the nature of spectroscopic techniques, spatial information is absent.

Overall, the following methods have shown potentials to be the tissue diagnostic tool:

- Fluorescence imaging
- Fluorescence lifetime imaging microscopy
- Narrow band imaging
- Autofluorescence imaging
- Bioimpedance
- Mass spectrometry
- Raman spectroscopy

- Diffuse Reflectance spectroscopy

For this project, **Diffuse Reflectance Spectroscopy (DRS)** was chosen as the tissue diagnosis modality, as it was most suitable for the engineering requirement derived from the needs of the surgeons. The **real-time spectroscopic data processing**, its **good resolution** being as small as a diameter of an optical fibre, **not requiring a pathologist**, **not requiring exogenous chemicals**, its **minimally invasiveness**, **easy calibration procedure** and **affordability** aspects of DRS were superior to other methods. More details can be found on Section 3.1 Requirement Analysis.

1.4 Diffuse Reflectance Spectroscopy (DRS)

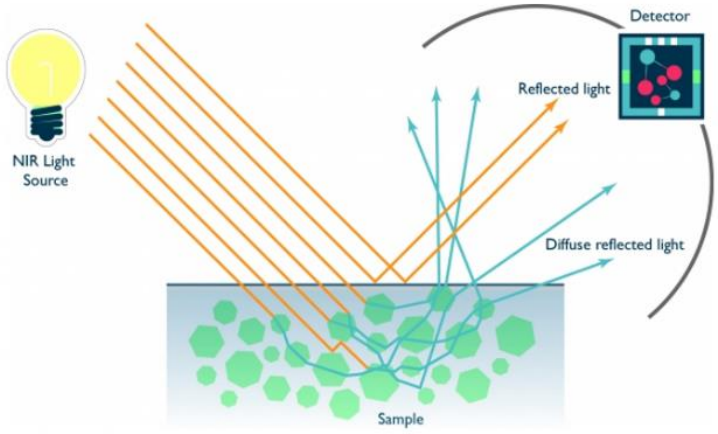

Figure 5 Diffuse reflectance light scattering [72]

Diffuse Reflectance Spectroscopy (DRS) is an optical spectroscopic technique that uses diffuse reflectance spectra as diagnostic tool. As shown on Figure 5, the reflectance spectra contain information about elastic light scattering and absorption from the tissue constituents, which can represent the morphological and physiological differences between different tissue types [73]. Previous studies have shown that DRS can be a promising modality for intraoperative margin assessment in brain, oesophageal, breast, colorectal, gynaecologic, skin cancer surgeries [27], [28], [70], [71], [74]–[82]. DRS has shown promising results in making quantitative spectral analysis beyond visible white light [28], [71], [76], [83], which are unperceivable by human eyes.

Figure 6 shows a noticeable development, ‘Endodrone’ by Avila-Rencoret *et al*, which combined a robotic actuation system with DRS to automatically screen for colorectal cancer and map tumour positions [71].

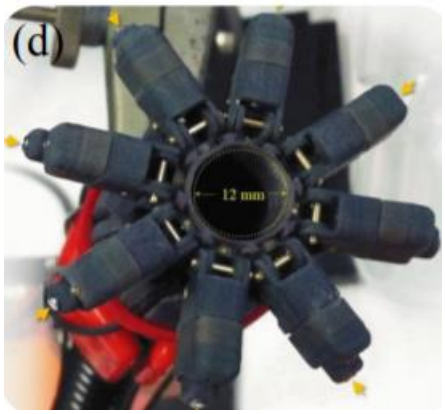

Figure 6 'Endodrone' by Avila-Rencoret *et al* [71]

DRS can be extremely useful in diagnosing epithelial cancers. According to Thiery *et al*, the generation of carcinoma at epithelial layer comprises of disruptive changes in cell morphology due to uncontrolled growth of cells [84], as shown on Figure 7. DRS can effectively detect these changes, as the scattering and absorption properties of the tissue will significantly change due to the morphological change of the epithelial tissues. Also, although clinical DRS generally only can penetrate a few mm at maximum [73], the epithelial tissue is generally thin enough that the DRS can detect the cancer beneath it easily.

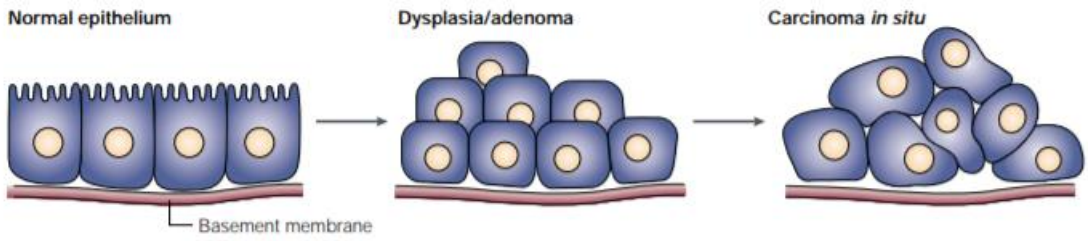

Figure 7 Generation of carcinoma at epithelial layer [84]

1.4.1 Fundamental Physics

To use DRS, understanding the process of producing diffuse reflectance spectra and how the spectra can represent morphological and physiological properties of the tissue is essential.

Photons can interact with tissue in four different ways: diffuse reflection, absorption, specular reflection and absorption by fluorophore [73]. Any non-absorbed light under the tissue surface undergoes multiple scattering and eventually emerges from the surface as diffuse reflectance.

Elastic scattering involves changing the photon's propagation direction. This takes place without loss of kinetic energy, hence no change of wavelength. Elastic scattering occurs due to changes in the refractive index in the travel path, for instance, nuclei, collagen fibrils, macromolecular aggregates etc. Scattering can occur in three different ways: Rayleigh scattering, Thompson scattering and Mie scattering [73]. Light is scattered more strongly in the forwards direction by tissue, in which its anisotropy of the scatter is determined by **"anisotropy coefficient" (g)**, which is the mean of the cosine value of angles that the light rays scattered. For tissues, g varies from 0.8-0.9 [73]. The **"scattering coefficient" (μ_s)** is the inverse of the average distance between scattering incidences. This scattering coefficient may change upon the degree of forward scattering as a new parameter **"reduced scattering coefficient" (μ_s')**, defined as:

$$\mu_s' = (1 - g)\mu_s \qquad \text{(Eq.1)}$$

Absorption occurs when the energy of an incident photon is being absorbed by an electron of a molecule within tissue to be promoted to a higher energy level. The principal absorbers in human tissue are melanin, fat, and haem group of haemoglobin. In particular interest, haemoglobin exist in two forms: **oxy-haemoglobin (HbO2)** and **de-oxy-haemoglobin (HHb)**, each having a distinctive absorption spectrum. The reflectance spectra will depend on **haemoglobin concentration** and **oxygen saturation**, which may vary by the size and number of blood vessels

and capillaries within the tissue sample. Using this, DRS can be used to detect cancerous tissues [85]–[90], since cancerous tissues can undergo sustained angiogenesis or hyper-metabolism, which suggests different local blood volume, blood oxygenation and tissue metabolism compared to normal tissues [91]. However, there are some exceptions in this method: small lesions size less than 2mm or hypo-vascular lesions can be difficult to detect as they have not experienced neo-angiogenesis [92]. The **"absorption coefficient"** (μ_a) is the inverse of the average distance a photon travels before it is absorbed. The coefficient for a tissue at certain wavelength can be described as:

$$\mu_a(\lambda) = 2.3 \cdot c \cdot [\alpha \cdot \varepsilon HbO_2(\lambda) + (1 - \alpha) \cdot \varepsilon Hbb(\lambda)] \cdot [CO_2]$$

(Eq.2)

where **c** is total haemoglobin concentration, **α** is the oxygen saturation coefficient, **εHbO2** and **εHbb** are the wavelength dependent extinction coefficients for oxyhaemoglobin and deoxyhaemoglobin respectively, and concentration of CO2.

The intensity from the incident light (I_o) decreases as a result of scattering and absorption, where the relationship is shown via a modified Beer-Lambert law:

$$\mathrm{I} = I_o e^{-\mu_{eff} z}$$

(Eq.3)

in which the $\mathbf{I_o}$ is the intensity of the incident light before any scatters or absorptions take place, **z** is the penetration depth, and $\boldsymbol{\mu_{eff}}$ is the "effective attenuation coefficient":

$$\mu_{eff} = \frac{1}{\delta}$$

(Eq.4)

where μ_{eff} is the inverse of the **"mean penetration depth" (δ)**:

$$\delta = [3 \cdot \mu_a \cdot \mu_t]^{1/2}$$

(Eq.5)

where the **"total attenuation coefficient" (μ_t)** is the sum of absorption coefficient and scattering coefficient:

$$\mu_t = \mu_a + \mu_s{}'$$

(Eq.6)

Before every session, the system must be calibrated with a white standard and readings for dark noise must be recorded. These values are used to normalise the spectra and remove noise. Once the spectra are normalised, the intensity can then be plotted out against the normalised wavelength of the spectra as shown on Figure 8.

$$\lambda_{normalised\ DRS} = \frac{(\lambda_{Raw} - \lambda_{Dark\ noise})}{(\lambda_{White\ standard} - \lambda_{Dark\ Noise})}$$

(Eq.7)

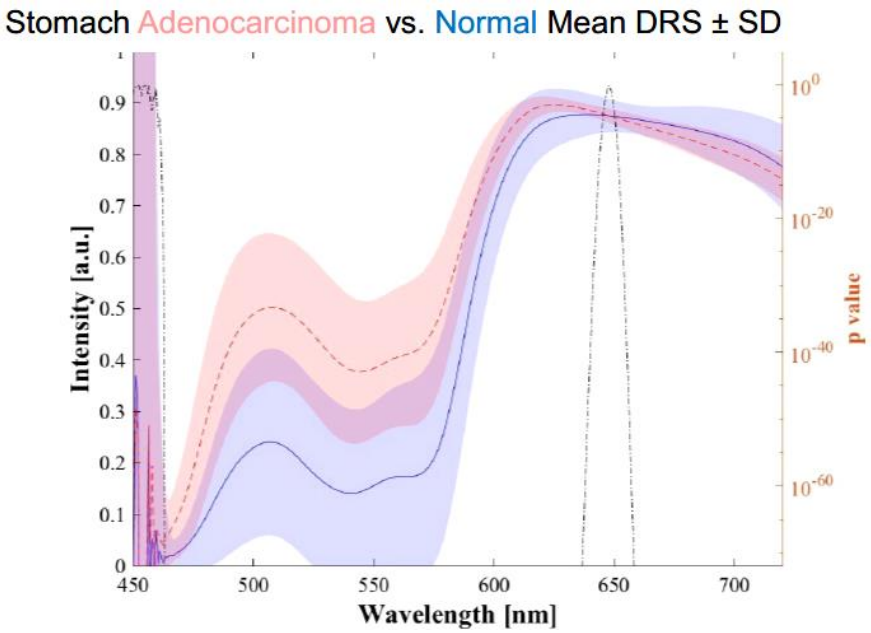

Figure 8 An example of DRS spectra of healthy tissues and cancer tissues [76]

The spectra that has been post-processed can then be classified into healthy tissue or cancerous tissue by machine learning techniques – Waldock *et al* and Avila-Rencoret *et al* had successful binary classification using support vector machine [42], [76].

1.4.2 Potential Advantages / Limitations of Margin Assessment using DRS

DRS has advantages over other intraoperative tissue diagnosis modalities for margin analysis purpose.

First: **DRS is minimally invasive and is non-ionising**, therefore the patient receives minimal trauma. This shows a great advantage over modalities like positron emission tomography or mass spectrometry, which exerts radiation exposure or tissue damages during the tissue diagnosis process.

Second: **Real-time data acquisition and classification** allows easy ergonomics of the system. Also, it does not add any delays to the total time taken for the surgery.

Third: the system is **easy to build, and cheap**. The system generally is comprised of a light source that has a wide spectrum (e.g. halogen arc lamp), a probe that consists of one or more optical fibres for delivery and collection of light, and a spectrometer and CCD camera to analyse the spectra [93], as shown on Figure 9. An example build costs $ 4,329 as shown in Table 2, which is significantly cheaper compared to other modalities, such as mass spectrometry being $ 380,000 [64], Raman spectroscopy system being $ 23,000 [94], and OCT being $ 50,000 [54].

Fourth: **The interpretation of the result does not require an expert**, since the quantitative spectroscopic data can be easily classified by using machine learning algorithms. Unlike optical coherence tomography, ultrasound, and confocal laser microscopy, DRS can be handled and perform data interpretation at the same time by the surgeon alone.

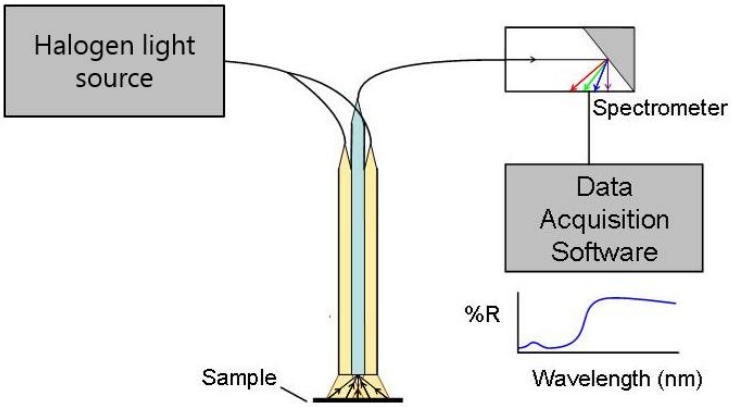

Figure 9 Spectroscope schematic [95]

Component model name	Description	Specification	Price
USB4000 Custom (Ocean Optics)	Spectrometer	Spectral resolution: ~0.1 – 10.0nm FWHM, USB 2.0	$2827 [96]
R200-7-VIS-NIR (Ocean Optics)	DRS probe	200 μm reflection probe, visible & near infrared	$495 [96]
HL-2000-HP (Ocean Optics)	Light source	Tungsten Halogen source, 360 – 2000nm, 1500h, 2960K, with 20W output	$917 [96]
		Total cost	$4239

Table 2 Price of DRS components

Fifth: **The manoeuvrability of the probe is excellent due to the probe's narrow cross-sectional area and small probe size**. This allows no occlusion within the field of view by the surgeon, which may be common in intraoperative environment.

Sixth: There is **no need to take physical sample**, hence preserving as much healthy tissues as possible, and eliminating sampling error. This shows advantage over frozen section, imprint cytology and mass spectrometry methods.

Seventh: **DRS does not require any preparation other than simple calibration using white standard**. Unlike fluorescence imaging, frozen section, or imprint cytology, there is no need to prepare pigment, dyes, or exogenous fluorophores to highlight cancerous tumours.

However, DRS also suffers from some limitations.

First limitation is that the **spectroscopic data does not comprise of spatial information.** With real-time data acquisition, the surgeon may diagnose the tissue below the probe and find out its class, however, the spatial information is lost once the probe changes its position. Wide-field imaging modalities, such as optical coherence tomography, fluorescence imaging etc does not suffer from this problem. **This limitation can be tackled by adding spatial information to the DRS readings**.

Second limitation is that a **stable probe-tissue contact is necessary for accurate DRS readings**. Many studies have shown evidences that stable spectra without any signal loss can only be achieved with a stable probe-tissue interface with appropriate pressure [97]–[102]. It is also shown that too much pressure compresses the blood vessels and cause reduced blood flow, therefore altering the metabolism of the tissue and density of light scatters [103], whereas too little pressure can fail to collect all the reflectance spectra [97]. **This limitation can be tackled by improving the probe design**.

Third limitation is that **the reflectance spectra indicates differences in constituents of the tissue underneath the probe, which may not be tumour specific**. The classification accuracy may suffer from inter/intra patient variability due to this. Also, in specific surgical scenarios, for example in case of presence of blood between the tissue surface and the probe, increases the total haemoglobin concentration in the reading. This causes false reading on the tissue characteristic, and potentially lead to misdiagnosis of the tissue as cancerous tissue, since cancerous tumours have higher total haemoglobin concentration compared to healthy cells [74], [86], [87]. **This**

limitation can be tackled by adopting additional modalities that may be cancer-specific, such as fluorescence spectroscopy etc.

Fourth limitation is that **the field of view of the probe is very small, therefore only local assessment of the margin is possible**. Although the location of tumours can be initially found by the preoperative imaging, there can be movement of the organs between the image acquisition and the surgery. Also, in case of generation of new tumour, or metastatic cancer movement towards nearby lymph node, DRS is not able to find out the change unless the surgeon scans over a large area which consumes a lot of time. **This limitation can be tackled by attempting to integrate other wide-field imaging techniques, such as hyperspectral camera [27], NBI or AFI.** The use of hyperspectral camera can be very well compatible with DRS, since both systems require broadband halogen light source, as well as CCD cameras with sensitivity at specific wavelengths, therefore sharing the equipment may reduce the total cost.

For this project, we focus on solving the first limitation by adding spatial information to DRS readings.

1.5 Spatial Data Fusion on DRS Data

Due to the nature of spectroscopic data, DRS data does not have any spatial information. This means that the surgeon cannot keep track of where he has performed tissue diagnosis on. There are two approaches in solving this:

First is to increase the field of view of the system, by installing more optical fibres in the core. This essentially makes the DRS system into a hyperspectral camera, which has shown a promising result in tissue diagnosis [27]. However, a wide-field imaging modality with a larger probe size may not have a good manoeuvrability, hence it does not suit with the proposed clinical solution.

Another way is to adopt a tracking system onto the probe, such that the **3D location of tissue diagnosis can be tracked in real-time**. The result of tissue classification can then be registered to the position, to provide a visualised tumour map in respect to the surgical scene for the surgeon. The surgeon can then use the tumour map as a visual guide to resect the tumour.

1.5.1 Tracking Modalities

There are number of ways to track a surgical instrument in intraoperative environment.

A vision-based approach uses RGB cameras to detect the surgical instrument within the camera's field of view (FOV). This is done by achieving a set of image features, then estimating the pose parameters from the features. Vision-based approaches are highly attractive, because there is no need of modification of the instrument of the operating theatre, as visualisation of tumour positions already requires an image data of the surgical scene from an RGB camera, regardless of the tissue diagnosis modality. Major problem for vision-based techniques is robustness, in particular to diverse range of surgical conditions that may affect image quality and visibility – wide range of appearance and lighting scenarios, shadow induction, occlusions, rapid appearance changes, smoke, specular reflections, blur, blood spatter etc. A way to improve the robustness is using fiducial markers like ArUco, which comprises of known feature sets [104].

Infrared optical approach uses a set of infrared cameras and infrared markers that reflect light of near-infrared wavelength around 900nm. Infrared optical approach is very similar to vision-based approach, except that the features that are used to estimate the pose, can be more easily derived as it is wavelength-specific [105]. Active markers like near infrared LEDs can be used along with two planar or three linear cameras, such that the pose can be estimated by triangulation. Passive markers can also be used in a similar way, but instead of active markers, at least three retroreflective spheres are illuminated by the infrared emitting cameras. Although not being widespread in medical applications, laser tracking system using arrays of photosensors is also possible [106]. However, infrared cameras tend to be more expensive than normal RGB cameras

due to incorporated band-pass filter, and infrared cameras cannot be used to visualise the tumour map, therefore an extra RGB camera is required in the surgery.

Electromagnetic approach uses disruptions within a known electromagnetic field caused by the movement of the sensor above the field generator. There are commercially available products that are compliant with many medical safety standards, such as Northern Digital Inc. Medical Aurora [107]. Although they are highly accurate, there is magnetic artifacts occurring when metallic object is placed above the field generator, which the probe may affect the tracking accuracy.

Robot kinematics approach uses the angle and translation information from the encoders between the links within the robot, and then use forward kinematic to calculate the pose of the end-effector. Well established surgical robots such as Intuitive Surgical DaVinci robot has shown its accuracy in kinematic tracking, however, these robots tend to be very expensive as they are designed for surgery, not for tracking. An attempt to use a cheaper alternative was done by the Project OpenPath [108] by using Phantom Omni [109], however, the project suffered from the small work volume of the robot.

Inertial measurement unit approach uses an inertial sensor that can measure acceleration in 6 degrees of freedom. Although the data acquisition rate is very high, evidences have shown that it suffers from drift problems [110].

Figure 10 Northern Digital Inc. Aurora [107], Figure 11 Optotrak Certus [111]

Figure 12 Intuitive Surgical DaVinci [112]

1.5.2 Temporal Tracking Methods

Temporal tracking is a method to link the measurements temporally to obtain a smoother trajectory [113]. By obtaining a smoother trajectory, the inherent accuracy error of the tracking modality can be reduced, and at times where the pose estimation has failed (e.g. heavy occlusion) it is possible to recover the correct pose by estimating the pose from smoothed trajectory.

There are three main ways of achieving temporal tracking:

The first method is by using sequential Bayesian filter, which estimates the optimal pose parameter at time t, given a measurement of it at t and the prior state at time t-1, based on

Bayesian statistics. A good example of Bayesian filter is Kalman filter, which is a popular temporal tracking methods in motion analysis and robot tracking [114].

The second method is by using Particle filter. The principle of estimating the optical pose parameter based on the prior state is similar, however, unlike sequential Bayesian filter, particle filter does not assume that the sensor uncertainty is in gaussian distribution. The Condensation algorithm is popular in surgical instrument tracking due to its ability to track through occlusions [115].

The last method is called initialisation, which is to simply initialise the search for the next frame's detection at the location of the previous frame's detection.

2 Project Objective, Plan and Thesis Structure

The objective of this project is to solve the clinical problem that surgeons cannot carry out accurate intraoperative margin analysis during cancer surgery without the assistance of pathology lab. The proposed clinical solution replaces inefficient processes of the current intraoperative margin assessment methods, by equipping the surgeons an ability to carry out quantitative margin assessment themselves. This is achieved by adopting an accurate probe-tracking system onto the diffuse reflectance spectroscopy system, such that real-time tissue diagnosis data is registered with spatial information.

By the end of project, the minimum deliverable should include a working system comprising of diffuse reflectance spectroscopy with visualisation of tumour map derived from real-time tissue diagnosis and tracked probe measurements, designed based upon the analysed engineering requirement, should be presented. This system should be validated on an *ex-vivo* experiment. Extension work may include probe design improvements, temporal tracking implementation, adoption of additional tissue diagnosis modality.

Milestone	Task
1	Define engineering requirements
	2D detection & tracking
2	3D tracking
3	Multi-marker probe tracking
4	3D tracking with Multi-camera system
5	Probe-tip estimation
	Register DRS + Tracking
6	Visualisation of probe-tip tracking
7	*Ex-vivo* experiment validation

Table 3 Project milestone plan

The thesis divides the research content into two chapters: ‘Customer analysis’ and ‘System Development’. The ‘Voice of Customer Analysis’ chapter is based on the techniques within the Design for Six Sigma methodology for product development [39]. In this chapter, the clinical problems derived from literature is confirmed in real surgical scenes, the qualitative needs of surgeons are analysed, the analysed qualitative needs are then converted into quantitative engineering requirements, and based on it the research plan and success measures are constructed. The ‘System Development’ chapter involves technical developments of the system from the most basic aspect and gradually expand the features as more experimental successes are achieved. The expansion of features is to be continued until the minimum deliverables of the project is achieved, which is to build a working system.

3 Voice of Customer (VOC) Analysis

Although the literature review has allowed understanding of theoretical requirements of intraoperative margin analysis procedure and analysing numerous tissue diagnosis modalities and tracking modalities, the decision on the system component was not possible until the needs of the surgeons and the engineering requirement for the system were truly investigated.

Design for Six Sigma methodology states that **a successful product is not simply the best performing and the most affordable, however, it should satisfy exactly what the voice of customer (VOC) demands**, which can be variety of requirements such as ergonomics, product lifetime, maintenance etc. Therefore, it is essential to deeply analyse the VOC prior to developing any product or systems [39].

3.1.1 Confirmation of the concept with expert surgeons

To ensure that the opportunities for IMA process improvement shown from literatures apply the same at the real scene, a confirmation and feedback was needed from the expert surgeons. One colorectal cancer surgery was observed, and during the surgery, two surgeons and two assistants were interviewed.

The experts first agreed that the IMA process is very inefficient, causing idle time at the operating theatre. During the surgery, it was observed when the biopsy was sent to the pathology lab for analysis, the assistants left the theatre for a short break and the surgeons taking rest, until the biopsies came back to the theatre.

The experts also agreed that an in-house IMA technique will greatly reduce the total surgery time. However, the experts agreed that the system must be easy to use to reduce the learning curve.

3.1.2 Qualitative Analysis using Kano Modelling

The interview about the VOC was carried out after confirmation of the concept. The VOC was initially collected and analysed by Kano modelling method, which is a popular technique in industries to analyse their customer's needs [116]. Kano model breaks the VOC into three categories: Basic, Performance and Excitement quality factors.

Basic quality factor does not increase any customer satisfaction when implemented in the system. However, the customer dissatisfaction increases when it is not implemented.

Performance quality factor increases customer satisfaction if implemented in the system. On the other hand, the customer dissatisfaction increases when it is not implemented.

Excitement quality factor increases customer satisfaction if implemented in the system. There is no customer dissatisfaction even when not implemented in the system.

Basic	Performance	Excitement
• High accuracy • Sterile	• Smooth use • Large workspace • Miniaturisation	• Robust • Easy calibration • Long life-span • Cheaper

Table 4 VOC analysis by Kano modelling

Table 4 shows the combined opinions of the surgeons and the assistants. Accuracy of the system and sterility was considered as the 'must' factors of the system. To be compared with other IMA techniques, the competing criteria were selected to be real-time processing, workspace coverage and miniaturisation. Miniaturisation was emphasised as often during gastrointestinal surgeries, certain locations are difficult to reach, therefore a small device would be preferred. Excitement factors were generally suggested by the assistants, and most factors focus on taking care of the system outside the surgery. Based on Design for Six Sigma methods, it is important to reduce

customer dissatisfaction before improving customer satisfaction. Therefore, it can be said the highest emphasis to the lowest emphasis are given to the quality factors from the left to right.

3.1.3 Quality Function Deployment and importance rating

To give priorities in development, as well as determining the engineering requirements, Quality Function Deployment technique was used. QFD is another popular technique in industrial product development to convert qualitative VOC into quantitative engineering requirements.

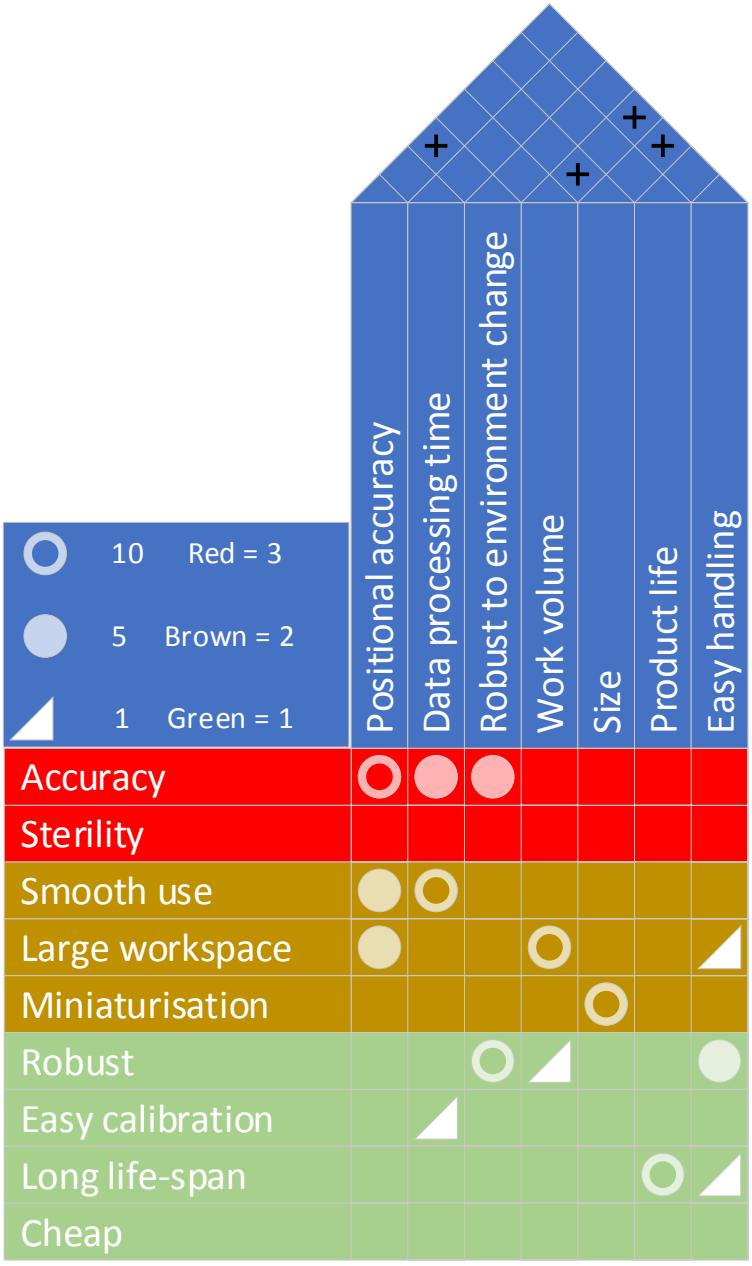

Figure 13 QFD-1 on VOC

Quality factors	Points	% of points
Positional accuracy	50	31.2
Data processing time	36	22.5
Robust to environmental changes	25	15.6
Work volume	21	13.1
Size	10	6.2
Product life	10	6.2
Easy handling	8	5.0

Table 5 Priority of development and importance distribution on success factors

Figure 13 shows the QFD diagram, where qualitative surgeon's needs are listed on the rows, and the engineering components that may be related to the surgeon's needs are listed on the columns. The basic quality factors are assigned with 3 x multipliers since they have the highest emphasis, and then performance quality factors are assigned with 2x multipliers, and excitement quality factors are assigned with 1 x multiplier (no multipliers). The central matrix is used to rate the link between the qualitative needs and the system component, which the strongest link has 10 points, middle link has 5 points, weak link has 1 point and no link has 0 points. The outcome of point calculations is shown on Table 5. It is important to note that the correlation matrix, which is above the column factors, have been marked but have not been included in the final calculation of the points. This is because only abstract data have been acquired – only 1 observation, the author has no experience in building similar system, no commercial products stating the exact engineering specification etc. Therefore, abstract QFD has been carried out.

3.1.4 Constructing Engineering Requirements

Generally, QFDs should go into deeper levels into QFD-2, QFD-3 etc, which then looks at quantitative values of each component. Generally, in the industry, the quantitative values are chosen based on the customer opinions, manufacturing policies and experiments on customer

satisfaction. However, **deeper levels of QFDs cannot be carried out in this case** for the following reasons:

- **Surgeons cannot give a collective expectation of the quantitative values**, as most surgeons do not have experience in variety of new IMA solutions, because they needed to follow the current gold standard.
- **There is no absolute guideline related to the quality factors by the government or the NHS**.
- **The project outreach does not allow for experiments on customer satisfaction** – only could barely observe 1 surgery.

Therefore, the quantitative engineering requirements just needed to be assumed, based on the previous literatures and surgeon's opinions. The engineering requirement is as shown on Table 6.

Quality factors	Quantitative values	% of points
Positional accuracy	Error < 1~2mm	31.2
Data processing time	> 5 fps	22.5
Robust to environmental changes	Light / shadows, temperature	15.6
Work volume	> 35 * 25 cm	13.1
Size	Miniaturisation	6.2
Product life	Long life span	6.2
Easy handling	Ergonomic features + Short calibration time (< 10 mins)	5.0
Sterility		Compulsory
Cheaper than other methods		Optional

Table 6 Engineering Requirements

3.2 Discussion and Further Work

VOC analysis is generally considered as a ‘must’ task in industries, as meeting the customer requirement is necessary in profit-making and it lets the developers understand the priorities in what aspect needs to be focused during the development. QFD is a great complementary technique to VOC analysis and is also highly recommended in industries to derive the engineering requirements.

Theoretically, the use of VOC + QFD can also bring an accurate assessment of customer requirement and produce a set of appropriate engineering requirements to meet the surgeon’s needs. However, for a successful implementation of VOC + QFD, a large set of qualitative opinions of the users are required, which has not been gathered for this project. This project assumed that the opinions of the surgeons are similar, since the previous literatures had similar arguments and opinions with the surgeons and assistants that were interviewed. Therefore, in the case of existence of different opinions, or different suggestions, the derived engineering requirement may not correctly represent the market (UK surgeons) needs.

To fix this issue and make improvements, a set of interviews for surgeons from different specialties and different hospitals may improve the accuracy of the engineering requirements. Also, exchanging ideas with a governmental association about cancer surgeries may be recommended, to establish a set of more accurate engineering requirements.

4 System Development

The system development chapter comprises of the idea generations, decision making and experiments for developing a working system. At this stage, the quantitative engineering requirement, as well as a list of tracking modalities were ready.

Robot kinematics method was firstly rejected as the tracking method. This is because small robots like the Phantom Omni used by Project OpenPath [108] was not suitable for the clinical workflow, due to its small work volume. Any large robots like Intuitive Surgical's DaVinci [112] may fit in the workflow, however, the budget for the project did not allow the use of DaVinci robots.

Infrared optical tracking method was also rejected, due to the expense of the system. Although infrared optical tracking ensures a submillimetre accuracy, both active marker system (Optotrak Certus [111]) and passive marker system (Optitrak Motion Capture System [117]) were out of budget.

Electromagnetic tracking method was considered as a secondary option. Despite the well-known accuracy of the system, it was not possible to know if the metallic probe will give undesired magnetic field disruptions, therefore increasing positional error, unless attempted in real-life.

Inertial measurement method was also considered as a tertiary option, due to its infamous drift issues. Also, all the inertial measurement unit devices were occupied for other MRes projects.

Vision-based tracking approach was eventually chosen as the main method. One of the main reasons is that we can save cost of the system a lot, since we need a camera to provide RGB image that visualisation of the DRS data can be overlaid with. With vision-based approach, there is **no need to modify the operating theatre nor purchase new equipment**. Vision-based approach seemed that it may compliment the one of the advantages of DRS, which is its

affordability. Overall, **DRS + vision tracking system will be a very low-cost system**, which may be attractive to hospitals.

4.1 Pre-experiment decisions

Before delving into development, a brief strategy in building the system and its schematic should be made to keep a clear goal.

4.1.1 Marker-less Instrument Tracking vs Fiducial Marker Tracking

First decision to be made was whether to do surgical instrument tracking with or without fiducial marker tracking.

Marker-less instrument tracking is done by estimating pose parameters from extracted features from the surgical instrument within the FOV of the camera. The performance of pose estimation varies depending on what feature methods were chosen. The features include colour, gradient, texture, shape, motion/disparity and semantic labelling features. Different feature extractors achieve different understanding of the scene, as shown in Figure 14. In the recent days, there has been attempts in using convolutional neural network to detect the surgical instrument within the field of view, such that the pose of the tip can be extracted [118].

Figure 14 Different feature extraction methods on the same image - From left to right: original image, colour, gradient, texture, semantic labelling [113].

However, marker-less instrument tracking methods **suffers from low robustness under environmental variabilities** - shadows, lighting changes, specular reflection, occlusion, blood spatter can all affect the tracking performance. **The DRS probe has metallic surface, which may suffer from specular reflection** at times. Also, the DRS probe is a contact-based method,

therefore **the edges of probe must be occluded when the DRS data acquisition takes place**. Additionally, marker-less tracking works great on the surgical tools with a lot of visual features to grab from, for example, the laparoscopic instrument shown in Figure 15 comprises of many joints and lines, which can be used to estimate the pose. Whereas, **the DRS probe just looks like a metallic rod from the outside, therefore there is not much visual features to grab from**.

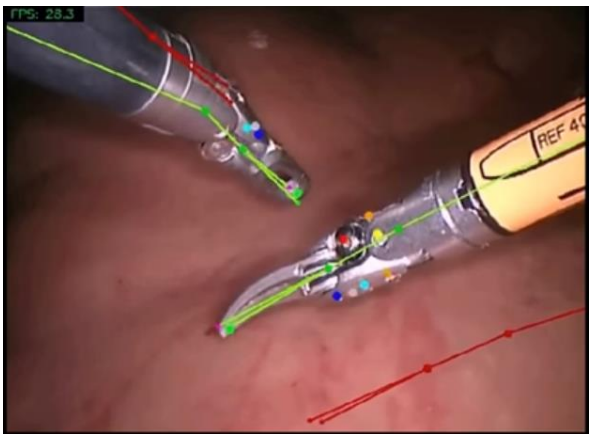

Figure 15 Example of marker-less surgical instrument tracking [119][120]

An alternative to marker-less tracking is by using fiducial marker tracking. A fiducial marker is basically a marker with a visually easily distinguishable features, therefore it is **more robust in environmental changes compared to marker-less tracking methods**. However, **probe tracking using fiducial marker tracking is a secondary tracking method**, because only the pose of the fiducial marker will be tracked, so extra calculations are required to transform the pose from the fiducial marker to the probe-tip. Also, fiducial markers take space, therefore **increase in the size of the probe device** is expected, and on the top of that, **the fiducial markers also suffer from occlusions**, so there is a restriction in positioning the fiducial marker at a easily visible place, which may not be optimal for ergonomic surgery.

Eventually, **fiducial marker tracking was chosen for the project**, because the probe does not have much visual feature, so additional features were needed for a stable pose estimation.

However, it is still desirable to minimise the marker size, so high manoeuvrability and large work volume can be achieved.

4.1.2 Selection of Libraries

There are many fiducial marker libraries out on the internet for example ArUco [104], ARToolKit [121], as well as those specifically designed for minimally invasive surgeries [122]. Despite the hybrid cylindrical fiducial marker designed by Zhang *et al* may occupy smaller volume, therefore leading to smaller probe device with better manoeuvrability and larger work volume, but the marker library was written in C++, and could not be wrapped into MATLAB [123] code to be used altogether with the DRS spectra acquisition code.

Eventually, ArUco marker library was chosen for the fiducial marker library due to its simplicity [104]. There are many versions of ArUco marker arrangements, such as Enclosed marker, Diamond ArUco marker, ChArUco board etc. Also, OpenCV, which is the parent library to ArUco library, was chosen to be used together with ArUco, for maximising efficiency in pose estimation [124].

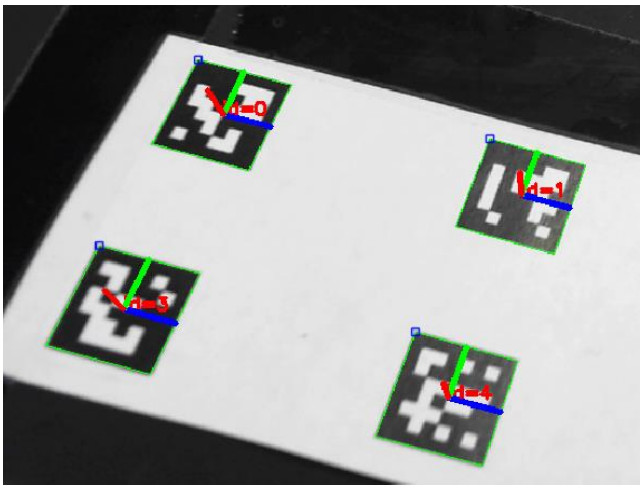

Figure 16 Example of an ArUco marker, Figure 17 Image of successful marker detection

OpenCV and ArUco libraries are originally written in C++, but a C++ to MATLAB interface for OpenCV, called ‘mexopencv’, could wrap the OpenCV functions to be used on MATLAB.

4.1.3 ArUco marker detection algorithm

ArUco marker detection comprises of a combination of simple image processing techniques. This means that the detection cannot happen simultaneously with image acquisition and can only begin once the image is saved in the memory. The algorithm is as follows:

1. Apply thresholding techniques (default: multi-level thresholding) to obtain borders
2. Find contours, so that only the borders of real markers remain in the image.
3. Remove borders with a small number of points.
4. Apply polygonal approximation of contour at the enclosed borders and find the 4 corner points. (Obtain edge vector)
5. Sort corners in anti-clockwise direction (Obtain corner information)
6. Remove too close rectangles.
7. Marker identification
    a. Remove the projection perspective using an homography, to obtain a frontal view.
    b. Apply Otsu's thresholding to binary classify the code.
    c. Identify the internal code.

4.1.4 ArUco marker pose estimation algorithm

Pose estimation of the marker is done by applying EPnP algorithm [125] on each of the edges of the ArUco marker, and then constructing a plane, of which the rotational vector and the translational vector in 3D space from the camera frame is calculated.

Prior to the EPnP algorithm, the camera must be intrinsically calibrated. The relationship of calibration matrix to the camera projection is as follows:

$$s\begin{bmatrix} u \\ v \\ 1 \end{bmatrix} = \begin{bmatrix} f_x & 0 & c_x \\ 0 & f_y & c_y \\ 0 & 0 & 1 \end{bmatrix} \begin{bmatrix} r_{11} & r_{12} & r_{13} & t_1 \\ r_{21} & r_{22} & r_{23} & t_2 \\ r_{31} & r_{32} & r_{33} & t_3 \end{bmatrix} [X \quad Y \quad Z \quad 1]' \tag{Eq.8}$$

, where (X,Y,Z) are the 3D coordinate points in the world space, (u,v) are the projection points, and the 3x3 matrix is the camera matrix of intrinsic parameters. The camera matrix contains information about f_x and f_y, which are the focal lengths in terms of pixel units, and (c_x, c_y), which represents the image centre [124].

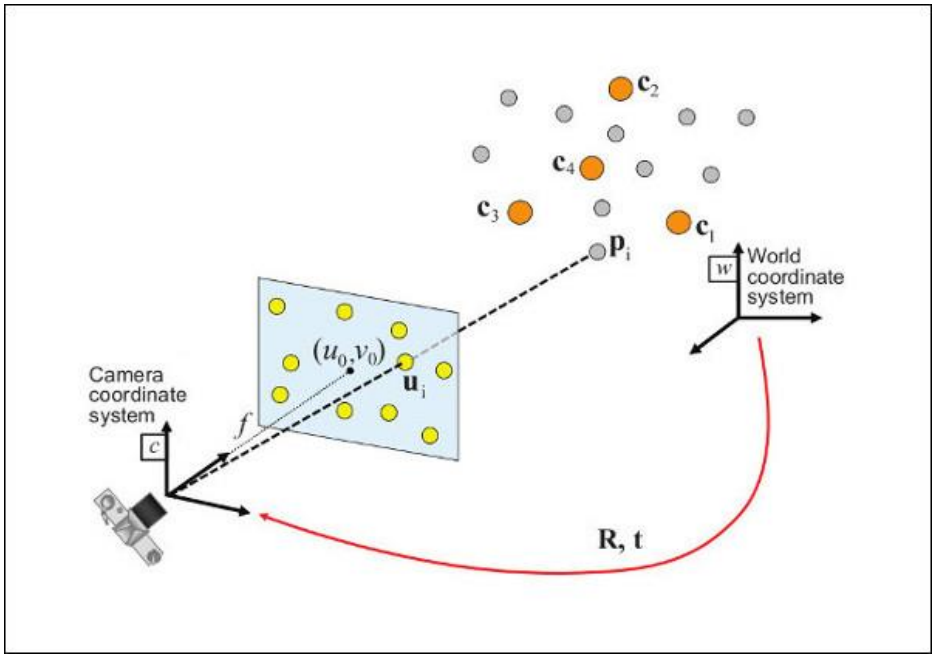

Figure 18 ePnP visual aid

ePnP solves the problem of Perspective-n-point problem by assigning four virtual control weight points onto every reference point. But in a simple explanation, 3D coordinate estimation from 2D projection is performed by using the camera matrix, as shown in Eq.9,

$$\begin{bmatrix} u \\ v \\ 1 \end{bmatrix} = \begin{bmatrix} f_x & 0 & c_x \\ 0 & f_y & c_y \\ 0 & 0 & 1 \end{bmatrix} \begin{bmatrix} 1 & 0 & 0 & 0 \\ 0 & 1 & 0 & 0 \\ 0 & 0 & 1 & 0 \end{bmatrix} \begin{bmatrix} r_{11} & r_{12} & r_{13} & t_x \\ r_{21} & r_{22} & r_{23} & t_y \\ r_{31} & r_{32} & r_{33} & t_z \\ 0 & 0 & 0 & 1 \end{bmatrix} \begin{bmatrix} X_w \\ Y_w \\ Z_w \\ 1 \end{bmatrix}$$

(Eq. 9)

and then the algorithm tries to minimise the reprojection error between the world reference points, (X_w, Y_w, Z_w), and the corresponding actual image points(X_c, Y_c, Z_c) by using Gauss-Newton

algorithm [125]. Eventually, the 4x4 matrix comprising of rotation and translation relative to the camera frame can be calculated.

$$\begin{bmatrix} X_c \\ Y_c \\ Z_c \\ 1 \end{bmatrix} = \begin{bmatrix} r_{11} & r_{12} & r_{13} & t_x \\ r_{21} & r_{22} & r_{23} & t_y \\ r_{31} & r_{32} & r_{33} & t_z \\ 0 & 0 & 0 & 1 \end{bmatrix} \begin{bmatrix} X_w \\ Y_w \\ Z_w \\ 1 \end{bmatrix}$$

(Eq. 10)

The ArUco pose estimation from the code included in this thesis gives the rotation values in Euler angles. This is done by extracting the 3x3 rotation matrix from the 4x4 matrix comprising of rotation and translation using cv.Rodrigues function [126], and then described in the form of Eq. 11 to maintain the same convention as OpenCV calculations. By resolving the subsidiary R values shown in Eq. 12, the rotation is described as ***rvec*** in Euler angles, and translation is described as ***tvec*** .

$$\mathrm{R} = \mathrm{Rz} * \mathrm{Ry} * \mathrm{Rx}$$

(Eq. 11)

$$\mathbf{R_x} = \begin{bmatrix} 1 & 0 & 0 \\ 0 & \cos(\theta_x) & -\sin(\theta_x) \\ 0 & \sin(\theta_x) & (\cos\theta_x) \end{bmatrix} \quad \mathbf{R_y} = \begin{bmatrix} \cos(\theta_y) & 0 & \sin(\theta_y) \\ 0 & 1 & 0 \\ -\sin(\theta_y) & 0 & (\cos\theta_y) \end{bmatrix} \quad \mathbf{R_z} = \begin{bmatrix} \cos(\theta_z) & -\sin(\theta_z) & 0 \\ \sin(\theta_z) & (\cos\theta_z) & 0 \\ 0 & 0 & 1 \end{bmatrix}$$

(Eq.12)

4.1.5 System Pipeline

With the ArUco marker detection and pose-estimation available, the system flowchart can be constructed.

Initially, the raw RGB image can be obtained from RGB camera, and the raw reflectance spectra can be obtained by the DRS probe. However, the raw inputs cannot be used for any useful

processing unless calibrated, so for the camera we use a calibration board and for the DRS probe we use a white standard to calibrate.

From the calibrated image and the camera intrinsic matrix, we can detect the ArUco marker and estimate the pose from it. Combined with pre-determined geometry between the ArUco marker to the probe-tip, the probe-tip position can be estimated.

For the DRS spectra acquisition, the calibrated spectrogram can be processed by a pre-trained machine learning classifier, which will tell if the tissue under the probe is healthy tissue or not.

By registering the temporal information of the DRS acquisition and the ArUco tracking acquisition, the fusion of DRS data and spatial information is complete.

Registering the tissue diagnosis data with spatial information to the calibrated RGB image, the probe measurement can be visualised.

For a fast repetition of this process, real-time tissue diagnosis may be possible.

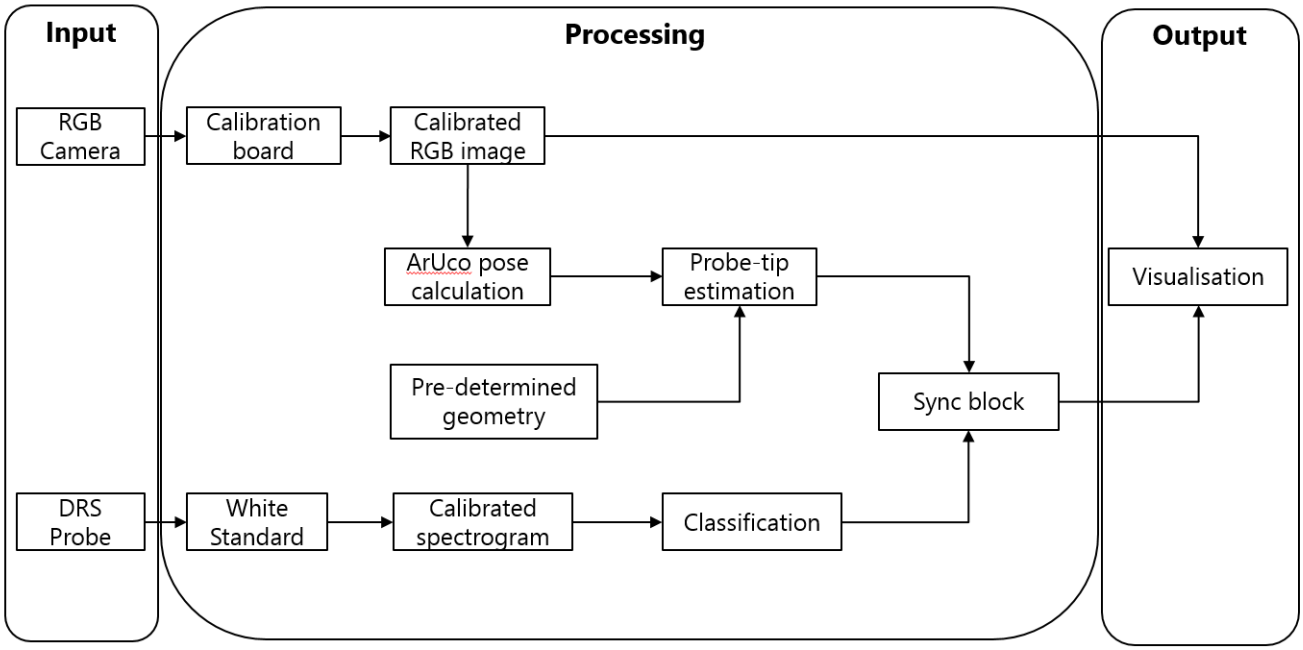

Figure 19 System flowchart

4.2 Methods

In this section, the methods of all the experiments in attempts to confirm the functionality, to seek for improvement opportunities, to fix errors, and to improve the system in overall. The experiments are listed in the order of process order.

The equipment used for the experiments are as follows:

- Laptop – CPU: Intel Core i7 4850HQ 2.30GHz, RAM: 16Gb.
- Camera (Old) – Microsoft VX-700
    - Resolution: 640 x 480
    - Fixed focus
- Camera (New) – 2 x Microsoft LifeCam Studio
    - Resolution: upto 1920 x 1080
    - Autofocus, Autoexposure, Auto-white-balance.

Figure 20 Microsoft VX-700 (Old), Microsoft LifeCam Studio (New)

4.2.1 Calibration Method

For an accurate pose estimation of the ArUco marker, an accurate and robust camera matrix and distortion model is required. In this experiment, four different calibration methods from MATLAB, OpenCV, ChArUco, which is a subsidiary library under ArUco library, and random SIFT pattern calibration method have been compared.